Quantitative Analysis of Relationship Between Pore Structure and Compressive Strength of Foamed Concrete

Geng Fei[1,2*], *Yin Wanyun*[3], *Xie Jianguang*[1], *Liu Shoucheng*[3], *Li Haoran*[1], *Gui Jingneng*[1]

1. College of Aerospace Engineering, Nanjing University of Aeronautics and Astronautics, Nanjing 210016, P. R. China;
2. School of Civil Engineering, Southeast University, Nanjing 210019, P. R. China;
3. China MCC17 Group Co., LTD, Maanshan 243000, P. R. China

(Received 17 October 2016; revised 10 January 2017; accepted 23 February 2017)

Abstract: The effect of dry density, water-cement ratio, the addition of fly ash, and sand content on the porosity and pore distribution of foamed concrete is investigated. Digital microscopy and Image J software are employed to examine the landscape of pores with different sizes. Based on the Balshin empirical formula, a mathematical model is established to quantitatively predict the relationship between the pore structures and the compressive strength of foamed concrete. The results well demonstrate that there is a significant correlation between the modified formula and empirical parameters.

Key words: foamed concrete; porosity; pore size; compressive strength

CLC number: TU551 **Document code**: A **Article ID**: 1005-1120(2018)03-0556-09

0 Introduction

Foamed concrete is a kind of heterogeneous material with high porosity. It has been widely applied in the engineering field due to its appealing properties of thermal insulation, earthquake resistance, fire resistance, and sound insulation[1]. Ideally, the pores of foamed concrete should be disconnected from one another, with uniform pore size and even distribution in the matrix. Under real circumstances, however, the size and distribution of pores are normally not uniform in the foamed concrete. As a result, the properties of foamed concrete are adversely affected, especially the compressive strength.

Previous studies have mainly focused on the effects of porosity, pore structure, and raw materials on the properties of foamed concrete. For example, Kearsley et al.[2-5] investigated the effect of the porosity on the compressive strength of foamed concrete. And a mathematical model was developed to evaluate the relationship between the porosity and the compressive strength. Just et al.[6] also studied the microstructure of high strength foamed concrete. Abd et al.[7] proposed a mathematical model for predicting the compressive strength of the lightweight foamed concrete. Hilal et al.[8] investigated the effect of different additives on the strength development of foamed concrete by characterizing the size and shape of air-voids.

Generally, the following four empirical formulas[9-10] are used to correlate the material porosity with the compressive strength of cement-based materials. However, they can only be applied to concrete with an average porosity. For the concrete with a high porosity, such as foamed concrete, they are not accurate and thus have to be modified.

$$f_c = f_{c,0}(1-n)^m \quad \text{(Balshin)}$$

* Corresponding author, E-mail address: gengfei@nuaa.edu.cn.

How to cite this article: Geng Fei, Yin Wanyun, Xie Jianguang, et al. Quantitative analysis of relationship between pore structure and compressive strength of foamed concrete[J]. Trans. Nanjing Univ. Aero. Astro., 2018,35(3):556-564.
http://dx.doi.org/10.16356/j.1005-1120.2018.03.556

$$f_c = f_{c,0} e^{-an} \quad \text{(Ryshkevitch)}$$

$$f_c = b \ln\left(\frac{n_0}{n}\right) \quad \text{(Schiller)}$$

$$f_c = f_{c,0} - cn \quad \text{(Hasselmann)}$$

where f_c is the compressive strength of concrete when the porosity equals to n; $f_{c,0}$ the compressive strength of concrete when the porosity equals to 0; n the porosity of the concrete; n_0 the porosity of concrete when the compressive strength equals to 0; and m, a, b, and c represent the empirical parameters.

Foamed concretes with different dry densities, water-cement ratios, sand contents and fly ash contents were prepared. The corresponding compressive strength of the prepared samples was evaluated. In addition, the inner pore structures of foamed concretes were examined and analyzed by employment of digital microscopy and Image J software. Consequently, the quantitative relationship between the pore structures and the compressive strength of foamed concretes was established by developing a mathematical model based on the Balshin empirical formula.

1 Material and Methods

1.1 Material

An ordinary Portland cement (OPC) with a 28-day strength of 50.0 MPa and grade I Fly ash (FA I) were used as cementitious materials. Grade II river sand with a fineness modulus of 1.9 was adopted as fine aggregates. A self-developed high-stability GL-2 foaming agent was employed to produce the foamed concrete. The properties of all these raw materials are shown in Tables 1—4 separately.

Table 1 Properties of cement

Specific surface area/($m^2 \cdot kg^{-1}$)	Normal consistency/%	28-day compressive strength/MPa	SO_3/%	MgO/%	Alkali content(R_2O)/%
370	28.0	50.0	2.14	1.50	≤0.60

Table 2 Properties of fly ash

Fineness 45 μm/%	Water demand ratio /%	Water content/%	SO_3/%	f-CaO/%	Activity index	
					7 d	14 d
3.20	87.00	0.24	0.88	0	86.00	109.00

Table 3 Properties of sand

Apparent density/($kg \cdot m^{-3}$)	Bulk density/($kg \cdot m^{-3}$)	Void fraction/%	Fineness modulus	Mud content/%	Chloride content/%
2 550	1 570	38	3.0	1.0	0.007 4

Table 4 Properties of GL-2 foaming agent

Foaming multiple	1 h exudation rate/%	1 h sedimentation distance/mm
42.2	38.1	4.3

1.2 Testing method

The slurry volume of all foamed concrete samples is equal according to the total mass principle. Foamed concrete samples (100 mm × 100 mm × 100 mm) with different mix proportions were prepared. According to "Foamed concrete" (JG/T266-2011), the dry density and compressive strength of hardened foamed concrete were evaluated by digital microscopy in order to observe the internal structure, while the pore structure was observed and analyzed by Image J and Photoshop software. The average pore diameter and the numerical fitting of aperture, porosity, and compressive strength were determined accordingly.

2 Characterization and Analysis of Pore Structure in Foamed Concrete

2.1 Internal pore structure of foamed concrete

(1) The pore structure of foamed concrete with various dry densities

As shown in Fig. 1, the pore sizes of foamed concrete with different dry densities were distinctive, which was a function of the dry density value. The porosity and pore size decreased with an increase in the dry density. It can be seen from Fig. 1(a) that grade 400 foamed concrete with a water-cement ratio ($R_{w/c}$) of 0.58, in which the slurry fluidity achieved even foaming, possessed closed spherical pores with a relatively larger diameter (0.516 9—0.554 3 mm). In contrast, grade 600 foamed concrete with the addition of 40% fly ash and a water-cement ratio of 0.44, in which the interim foam was accumulated, displayed a larger volume of uniformly distributed pores with a medium size (0.312 7—0.412 7 mm) due to the fly ash induced adsorption of foams (Fig. 1(b)). Fig. 1(c) showed that grade 1 000 foamed concrete ($R_{w/c}=0.44$) with the addition of 20% fly ash and a 20% sand had a lower proportion of spherical pores compared with the other density grades samples. It should be noted that although the pores of grade 1 000 foamed concrete had smaller apertures and were more evenly distributed due to the fly ash induced absorption and the friction caused by sand, deformation of some of the foam structures was observed.

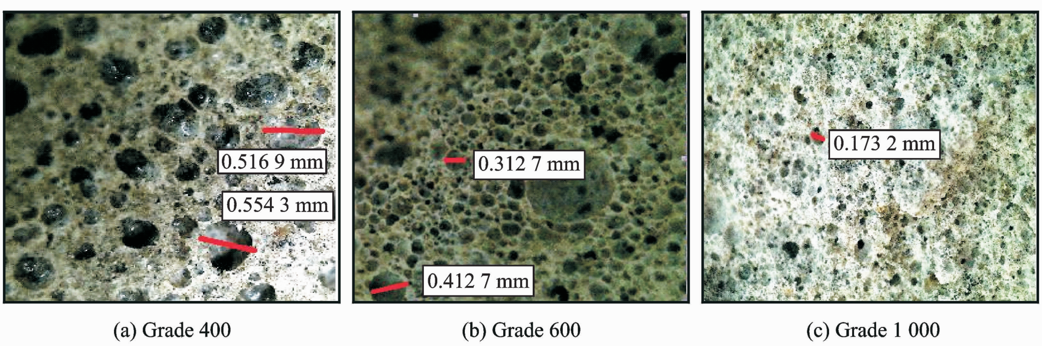

Fig. 1 Pore structures of foamed concrete with different dry densities

(2) Internal pore structure of foamed concrete with different water-cement ratios

It can be seen from Fig. 2 that foamed concretes with different dry densities successfully obtained cavity structures based on optimum water-cement ratios. At a lower water-cement ratio, the mixtures were prone to undergoing pore deformation during the mixing process due to the samples with a higher viscosity and uneven stress, resulting in poor pore structures. For example, grade 400 foamed concrete with a water-cement ratio of 0.54 generated a large volume of air bubbles. However, these bubbles were not well dispersed because of the high viscosity of the slurry. As a result, interconnected pores were formed. Increasing the water-cement ratio was conducive to producing uniform spherical pore structures with relatively large pore sizes, particularly for grades 400—600. And there was a corresponding increase in the amount of foams with a larger pore size. However, the downside of increasing water to cement ratio was an accompanying decrease in both the evenness of pore size and the compressive strength of the hardened samples.

(3) Internal pore structure of foamed concrete with different cement-sand ratios

Fig. 3 showed that the internal pore structures of foamed concrete gradually deteriorated through increasing the sand quantity. The incorporation of sand in foamed concrete plays a decisive role in influencing the compressive strength of foamed concrete. A higher sand proportion led to an increased friction within the inner slurry and thereby damaged the foam structure, causing some foams to burst. Moreover, increasing the sand content proportionately reduced the amount of cementing materials, thus reducing the volume of encapsulated foam slurry and thereby causing the unattached bubble to be connected. A cement-sand ratio ($R_{c/s}$) of 1 : 14 was found to be advantageous in pore structure formation, whereas some deformation ensued due to the increased friction. At a cement-sand ratio of 1 : 16, the pore connectivity began to appear, and the pore size increased. As the cement-sand ratio continued to increase, so was the pore connectivity. At a cement-sand ratio of 1 : 18, pore structures varied significantly, manifesting an irregular polygon shape. At such a high ratio, spherical pores became indistinguishable while the connectivity of the pores became harmful when the size of pores reached a diameter of above 1 mm.

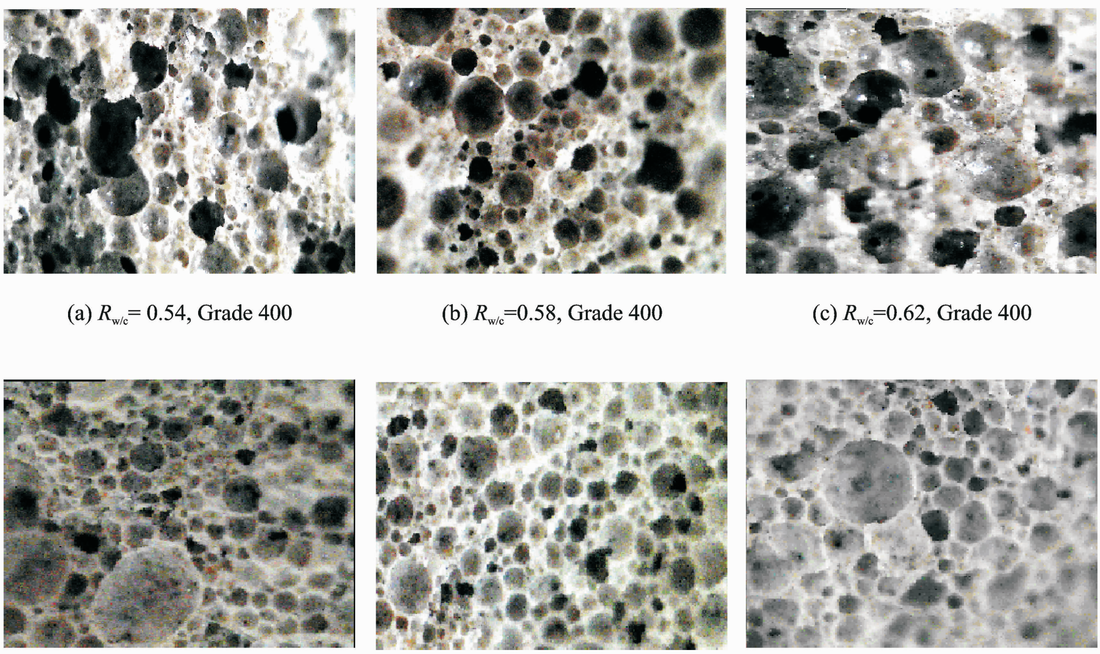

(a) $R_{w/c}$= 0.54, Grade 400 (b) $R_{w/c}$=0.58, Grade 400 (c) $R_{w/c}$=0.62, Grade 400

(d) $R_{w/c}$= 0.40, Grade 600 (e) $R_{w/c}$= 0.44, Grade 600 (f) $R_{w/c}$=0.48, Grade 600

Fig. 2 Internal pore structures of foamed concrete with different water-cement ratios

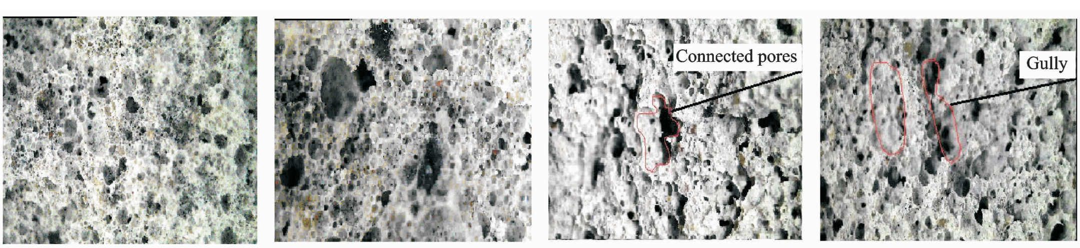

(a) $R_{c/s}$= 1:1.4 (b) $R_{c/s}$=1:1.6 (c) $R_{c/s}$=1:1.8 (d) $R_{c/s}$=1:2.0

Fig. 3 Internal pore structures of foamed concrete with different cement-sand ratios

2.2 Calculation of foamed concrete porosity and pore size

The internal pores of foamed concrete consisted of three parts: foams generated by foaming agents, a small amount of air, and pores incurred by water evaporation. Among them, foaming agents generated foams accounted for the largest proportion. During the hardening process of the foamed concrete, most of the free water took part in the hydration reaction, and bonded with the resulting products to stay in the cementitious matrix, while the rest of the free water had evaporated, leaving tiny pores in the matrix. Thus, the porosity of foamed concrete, n, equals to 1 minus the actual volume V_S, which is the volume occupied by the solid, as shown in Eqs. (1),(2).

$$n = 1 - V_S \tag{1}$$

$$V_S = V_c + V_W \tag{2}$$

where V_c is the volume ratio occupied by cement, and V_W the volume ratio of water participating in the hydration reaction.

The wet density of even slurry after mixing is written as ρ_h, hence V_S can be described as

$$V_c = \frac{\rho_h \times m_c}{(m_c + m_w) \times \rho_c} \tag{3}$$

$$V_W = \frac{\rho_h \times k m_c}{(m_c + m_w) \times \rho_w} \tag{4}$$

$$V_S = \frac{\rho_h (m_c \rho_w + k m_c \rho_c)}{(m_c + m_w) \rho_w \rho_c} = \frac{\rho_h (\rho_w + k \rho_c)}{(1+K) \rho_w \rho_c} \tag{5}$$

where m_c is the quantity of the cement slurry; m_w the quantity of water in slurry; ρ_c the apparent density of cement; ρ_w the density of water; k the lowest water-cement ratio required for completion of the hydration reaction, 0.20; and K the water-cement ratio during the preparation of foamed concrete.

Eq. (5) can be substituted into Eq. (1) to obtain the foamed concrete porosity n, which is shown as

$$n = 1 - \frac{\rho_h (\rho_w + 0.20 \rho_c)}{(1+K) \rho_w \rho_c} \tag{6}$$

Fig. 2 showed that foamed concrete with the identical dry density rating had pores of different varying sizes under different external conditions. The average size of pores had a significant impact on the mechanical properties of foamed concrete. Therefore, it is of great importance to evaluate the average pore size of foamed concrete prior to investigating the relationship between the pore structures and the compressive strength. Testing samples were collected from three cross-sectional areas (with smooth and neat surface) of the internal foamed concrete. The obtained samples were then analyzed by means of Image J software. The average chord length (L) of all the samples within the sampling range was calculated to obtain the average porosity of the three sampled cross sections. Then, the values were converted to the average pore diameter (r), which is shown as

$$r = L/\ 0.785^2 = L/0.616$$

Image J software was employed to measure the average pore diameters (r) of foamed concrete with different water-cement ratios and different grade dry densities. According to Eq. (6), the porosity (n) of the above samples was calculated, and the results are shown in Table 5.

Table 5 Average pore diameter and porosity of foamed concrete with different water-cement ratios and dry densities

P_{dry}/(kg·m^{-3})	$R_{w/c}$	r/mm	n/%
400	0.54	0.545	81.7
	0.58	0.521	82.1
	0.62	0.597	82.6
600	0.40	0.363	73.1
	0.44	0.328	73.9
	0.48	0.412	74.6
700	0.40	0.346	69.4
	0.50	0.301	71.4
	0.60	0.357	73.2
1 000	0.40	0.173	58.2
	0.44	0.181	59.4
	0.48	0.204	60.5

3 Mathematical Model of Pore Structure and Strength of Foamed Concrete

Foamed concrete with different water-cement ratios displayed various levels of dry densities. The porosity (n) and compressive strength of foamed concrete were analyzed. Fitting analysis was performed on the four mentioned empirical formulas, whose results are provided in Fig. 4.

As shown in Fig. 4, the Hasselmann correlation encountered limitations compared with other fitting formulas. The intensity of foamed con-

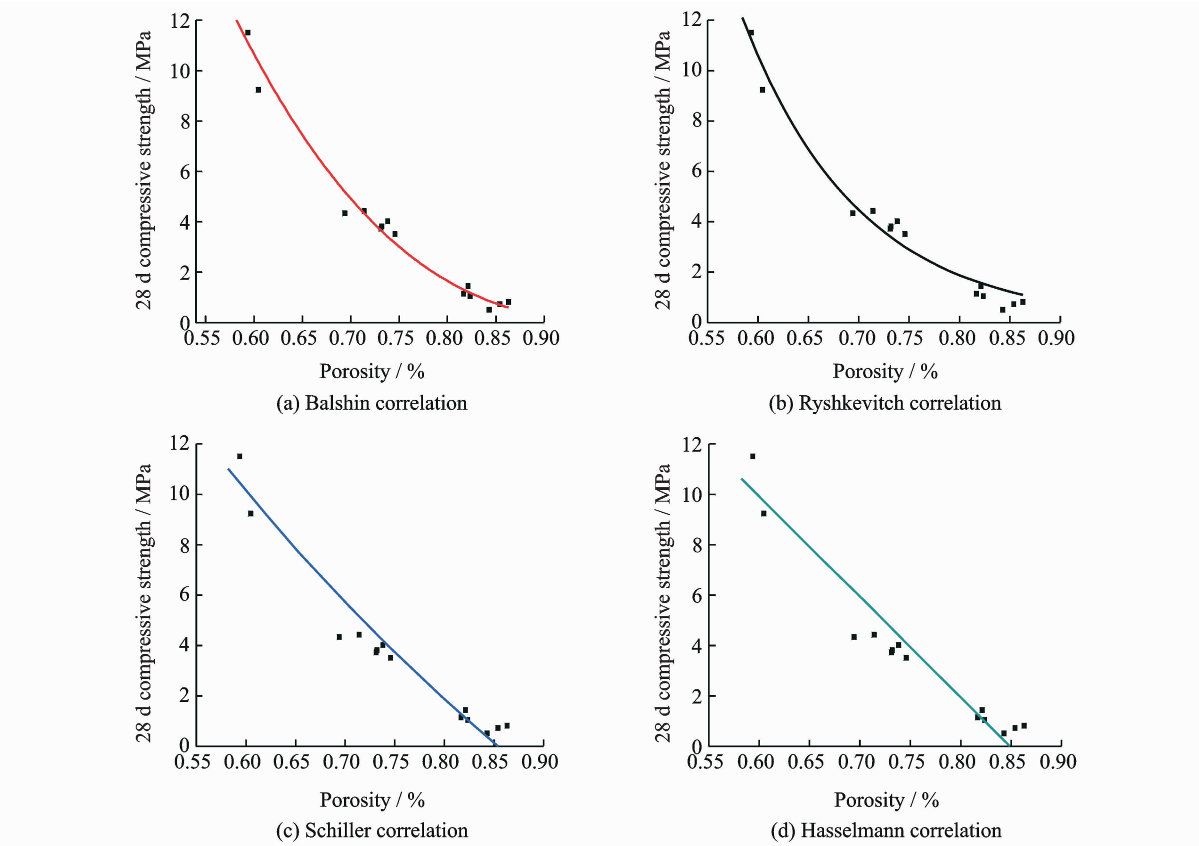

Fig. 4 Relationship and fit line between porosity of foamed concrete and compressive strength by four formulas

crete increased with a decrease in the porosity, although the fit did not show a linear attenuation. Moreover, when the porosity was in the range of 60%—80%, the change in the compressive strength was negligible. At a porosity of 10%—60%, the samples experienced some more obvious changes in compressive strength.

The fitting results demonstrated that the Balshin and Ryshkewitch formulas held advantages over the Hasselmann and Schiller formulas. To a certain extent, the relationship between the porosity and the compressive strength was accurately reflected by the Balshin and Ryshkewitch formulas. However, the four empirical formulas only considered the effect of the porosity on the compressive strength, and failed to take into account the influence of the pore distribution and the pore sizes. Thus, the compressive strength value of samples with the optimum water-cement ratio was higher than that of samples with a lower water-cement ratio. It should be noted that this fitting was not reflected in the current experiment. Thus, the use of the above four empirical formulas for single factor fitting and analysis was incomprehensive and subjective. For example, for grade 600 foamed concrete prepared with different water-cement ratios, although the basal porosity of those with a water-cement ratio of 0.44 was higher than that of those with a water-cement ratio of 0.40, the compressive strength of the latter sample was higher than that of the former one due to the presence of smaller pore sizes and more even pore distribution.

The fitting results of four empirical formulas are shown in Table 6.

Table 6 Equations for the 28 d compressive strength-porosity relationship of foamed concrete

Fitting function	Fitting equation	R^2
Power (Balshin)	$f_c=124.9(1-n)^{2.68}$	0.983 6
Exponential (Ryshkevitch)	$f_c=1\,874.5e^{-8.63n}$	0.980 2
Logarithmic (Schiller)	$f_c=28.8\ln(0.85/n)$	0.948 2
Linear (Hasselmann)	$f_c=33.7-39.7n$	0.922 8

The results indicated that when it comes to investigating the relationship between the pore structures and the compressive strength of foamed concrete, it is far insufficient to only take into consideration of the porosity. Tang et al.[11] established a mathematical model to predict the relationship between the compressive strength and the pore sizes of porous materials based on the Griffith fracture mechanics and composite material theory, which is shown as

$$\sigma_t = \sqrt{\frac{2E\gamma}{\pi C}} \tag{7}$$

where σ_t is the material critical fracture stress; C the half-length value of the crack; E the elastic modulus of materials; and γ the surface energy.

On the basis of the above model, Jin et al[12] deduced the relationship between E_c, γ, C, and r (pore radius). In addition, according to the material surface energy and porosity and research results of Kumar et al.[13-14] and Diamond[15], the relations could be obtained as

$$E_c = E_0(1-n),\quad \gamma_c = \gamma_0(1-n),\quad C = qn$$

where E_c is the elastic modulus at porosity n; E_0 the elastic modulus of the matrix; γ_c the surface energy at porosity n; γ_0 the surface energy of the material matrix fracture; and q the correlation coefficient of the pore shape.

The relationship between the critical stress of the material and the pore size can be obtained by introducing the above formula into Eq. (7), which is shown as

$$\sigma_t = \sqrt{\frac{2E_0\gamma_0}{q\pi}}\,\frac{1-n}{\sqrt{r}} \tag{8}$$

where $\sqrt{\frac{2E_0\gamma_0}{q\pi}}$ is determined by the strength of the cement matrix parameters, M. Matrix intensity is related to the total mass percentage of cement, as detailed in previous research by Kumar and Bhattachrjee[13]. Therefore, Eq. (8) can be amended as

$$\sigma_t = M_1 M\frac{1-n}{\sqrt{r}} = \frac{1}{1+K}M\frac{1-n}{\sqrt{r}} \tag{9}$$

where M_1 is the percentage of cement in the total quantity and K the water-cement ratio.

As shown in Table 3, the compressive strength of foamed concrete did not decrease with increasing the porosity in a linear manner, although there was a linear relationship between the compressive strength and the porosity and average pore size after the formula was amended. Furthermore, the fitting range of the Balshin and Ryshkewitch equations was more accurate when the four empirical formulas were combined with Eq. (9) to describe the relationship between the critical stress, porosity, pore size, and water-cement ratio. The Balshin and Ryshkewitch equations after amendment are shown as

$$f_c = f_{c,0}\left(\mu\frac{1-n}{1+k}\frac{1}{\sqrt{r}}\right)^m \tag{10}$$

$$f_c = f_{c,0}\exp\left(-\mu\frac{1-n}{1+k}\frac{1}{\sqrt{r}}\right) \tag{11}$$

Formulate $(1-N)/(1+K)$ and average pore diameter r as described by Eqs. (10), (11) were set as the independent variables. Then, the f_C curved surface was fitted, whose results are shown in Fig. 5.

The fitting equation can be described as

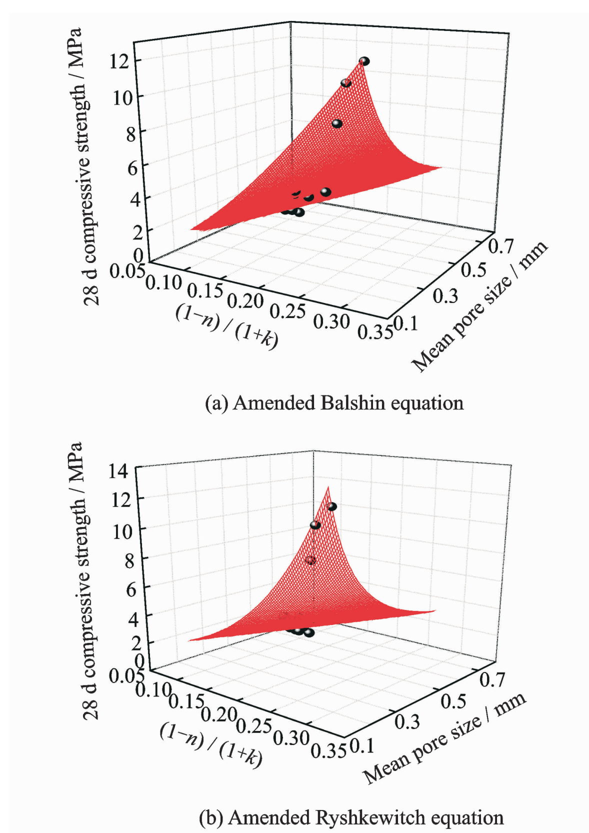

Fig. 5 Surface fitting for porosity and average pore diameter with 28 d compressive strength foamed concrete by two different equations

$$f_c = 13.14\left(1.39\frac{1-n}{1+K}\frac{1}{\sqrt{r}}\right)^{1.52} \quad R^2 = 0.9881 \tag{12}$$

$$f_c = 1.04\exp\left(-3.67\frac{1-n}{1+K}\frac{1}{\sqrt{r}}\right) \quad R^2 = 0.9661 \tag{13}$$

As shown in Eqs. (10), (11), for foamed concrete prepared only with cement, water, and foam, the experimental data and the fitting range were more accurately fitted with each other after the equations were amended. The traditional empirical formula is typically used to reflect the compressive strength and porosity of the raw cement materials. Thus, it suffers certain limitations when external conditions change because the corresponding empirical constants will occur concurrently. The application range was greatly expanded by amending the formulas to include the effects of porosity, average pore size, and water-cement ratio.

When the water-cement ratio K was fixed, the compressive strength of foamed concrete was determined by the porosity n and the average pore radius r. In other words, the compressive strength increased as the porosity and pore size decreased. When the porosity n was fixed, the compressive strength was determined by the water-cement ratio and the average pore radius. When the dry density of foamed concrete was fixed, its compressive strength was determined by both the matrix strength and the pore structure if the material only consists of cement, water and foam. Low water-cement ratios resulted in comparatively larger $1/(1+K)$ values, thus degrading the pore structures. Meanwhile, $1/\sqrt{r}$ will also be decreased if the viscosity and fluidity was not well controlled. Therefore, it is not advisable to consider only increasing the matrix strength without taking into account the effect of changes in the pore size on the compressive strength of foamed concrete.

4 Conclusions

(1) The average pore size of foamed concrete increased with the decrease of dry density levels.

(2) The average pore size of foamed concrete varied greatly as the water-cement ratio increased or decreased from the optimal ratio. Moreover, high cement-sand ratios had a significant impact on the performance of foamed concrete. At a higher mortar ratio, the foamed concrete suffered a degradation in the pore structures and had more interconnected pores.

(3) Among the four different types of porosity and empirical strength equations, the Balshin formula was found to be the best fit.

(4) The results, $f_c = 13.14\left(1.39\frac{1-n}{1+K}\times\frac{1}{\sqrt{r}}\right)^{1.52}$ and $f_c = 1.04\exp\left(-3.67\frac{1-n}{1+K}\frac{1}{\sqrt{r}}\right)$, were obtained by amending the Balshin and Ryshkewitch formulas. The surface bend fitting formula amended by Balshin had the best correlation ($R^2 = 0.9881$). The fitting equation was $f_c = 124.9(1-n)^{2.68}$, in which $R^2 = 0.9836$.

(5) The compressive strength of foamed concrete was mainly related to the matrix strength and characteristics of pore structures. However, the effect of water-cement ratio, slurry flow, and viscosity on the pore structures should also be taken into consideration.

Acknowledgements

This work was supported by the National Science & Technology Pillar Program during the Twelfth Five-Year Plan Period (No. 2015BAL02B02), the Jiangsu R & D Project of Modern Agriculture (No. BE2015349), and the China MCC "three five" Major Science and Technology Projects (MCC, [2013]1).

References:

[1] ZHAO G Z. Performance and advantages of the foamed concrete[J]. Fujian Building Materials, 2011 (3):21-25.

[2] KEARSLEY E P, WAINWRIGHT P J. The effect of high fly ash content on the compressive strength of foamed concrete[J]. Cement and Concrete Research, 2001,31(1):105-112.

[3] KEARSLEY E P, WAINWRIGHT P J. Ash content for optimum strength of foamed concrete[J]. Cement and Concrete Research, 2002,32(2):241-246.

[4] KEARSLEY E P, WAINWRIGHT P J. The effect of porosity on the strength of foamed concrete[J].

Cement & Concrete Research, 2002,32(2):233-239.

[5] KEARSLEY E P, WAINWRIGHT P J. Porosity and permeability of foamed concrete[J]. Cement and Concrete Research, 2001,31(5):805-812.

[6] JUST A, MIDDENDORF B. Microstructure of high-strength foam concrete[J]. Materials Characterization, 2009,60(7):741-748.

[7] ABD A M, ABD S M. Modelling the strength of lightweight foamed concrete using support vector machine (SVM)[J]. Case Studies in Construction Materials, 2017,6:8-15.

[8] HILAL A A, THOM N H, DAWSON A R. On void structure and strength of foamed concrete made without/with additives[J]. Construction and Building Materials, 2015,85:157-164.

[9] RÖBLER M, ODLER I. Investigations on the relationship between porosity, structure and strength of hydrated portland cement pastes I. Effect of porosity [J]. Cement and Concrete Research, 1985,15(2):320-330.

[10] NAMBIAR E K K, RAMAMURTHY K. Influence of filler type on the properties of foam concrete[J]. Cement and Concrete Composites, 2006,28(5):475-480.

[11] TANG L. A study of the quantitative relationship between strength and pore-size distribution of porous materials[J]. Cement and Concrete Research, 1986, 16(1):87-96.

[12] JIN N G, JIN X Y, GUO J F. Relationship modeling of pore structure and strength of concrete[J]. Journal of Zhejiang University, 2005,39(11):1680-1684.

[13] KUMAR R, BHATTACHARJEE B. Porosity, pore size distribution and in situ strength of concrete[J]. Cement and Concrete Research, 2003, 33(1): 155-164.

[14] KUMAR R, BHATTACHARJEE B. Study on some factors affecting the results in the use of MIP method in concrete research[J]. Cement and Concrete Research, 2003,33(3):417-424.

[15] DIAMOND S. Mercury porosimetry—An inappropriate method for measurement of pore size distributions in cement-based materials[J]. Cement and Concrete Research, 2000,30(10):1517-1525.

Dr. **Geng Fei** received his M. S. degree in material science from Southeast University in 2001 and Ph. D. degree in highway and railway engineering from Nanjing University of Aeronautics and Astronautics (NUAA) in 2013. From 2004 to present, he worked as an assistant researcher at civil engineering experiment center of NUAA and entered the postdoctoral station of the civil engineering discipline of Southeast University in 2013. His main research interests include energy saving technology and materials for building, utilization of solid waste resources, and functional chemical building materials.

Prof. **Yin Wanyun** received his B. S. degree in industrial and civil architecture from Anhui Institute of Architecture and Industry in 1986, and M. S. degree in engineering mechanics from Southwest Jiaotong University in 1989. He was hired by Hefei University of Technology as a master's tutor in 2011. From 1989 to present, he worked in China MCC17 Group Co., Ltd. His main research interests include technological innovation, quality management, housing industrialization and so on.

Prof. **Xie Jianguang** received his B. S. degree in chemical equipment and machinery and M. S. degree in chemical process machinery from Tianjin University in 1999 and 2002, Ph. D. degree in material science and engineering from Southeast University in 2005. From 2005 to present, he has been working in the department of civil engineering of NUAA. His main research interests include subgrade and pavement engineering, new material & new process of road, construction & operation of low carbon highway and design & maintenance technology of airport pavement.

Mr. **Liu Shoucheng** received his B. S. degree in hydrogeology and engineering geology from Xi'an Geological Institute in 1995 and M. S. degree in industrial engineering from Hohai University in 2013. From 1995 to present, he worked in China MCC17 Group Co., Ltd. His main research interests include construction industry modernization, construction technology and quality control and so on.

Mr. **Li Haoran** received his B. S. degree in traffic engineering from Shandong University of Technology in 2009 and M. S. degree in highway and railway engineering from NUAA in 2014. His research interests include airport pavement repair and pavement new materials.

Mr. **Gui Jingneng** received his B. S. degree in civil engineering from NUAA in 2014. Now he is a postgraduate in NUAA. His research interests include the development and application research of light-weight building energy-saving materials.

(Production Editor: Wang Jing)